LASER INTERFEROMETER GRAVITATIONAL WAVE OBSERVATORY
-LIGO-
CALIFORNIA INSTITUTE OF TECHNOLOGY
MASSACHUSETTS INSTITUTE OF TECHNOLOGY

Technical Note **LIGO-T000134- 00- D** 8/00

Dynamical Properties of LIGO Single Loop Suspended Mirrors

M. Rakhmanov, D. Reitze, D. Tanner, S. Yoshida
and H. Yamamoto

This is an internal working note
of the LIGO Project.

Distribution of this draft:
LIGO

California Institute of Technology
LIGO Project - MS 18-34
Pasadena CA 91125
Phone (626) 395-2129
Fax (626) 304-9834
E-mail: info@ligo.caltech.edu

Massachusetts Institute of Technology
LIGO Project - MS NW17-161
Cambridge, MA 02139
Phone (617) 253-4824
Fax (617) 253-4824
E-mail: info@ligo.mit.edu

WWW: http://www.ligo.caltech.edu/

file /home/malik/docs/T000134.ps

Contents

1 Suspension Dimensions **3**

2 Types of Motion **4**
2.1 Degrees of Freedom 4
2.2 Planar Motion 5
2.3 Pure ϕ-rotations 7

3 Lagrangian for a Suspended Mirror **8**
3.1 Potential Energy 8
3.2 Kinetic Energy 8
3.3 Lagrangian 8
3.4 Equations of Motion 9

4 Eigen-Modes of Mirror Oscillations **10**
4.1 Calculation of Eigen-Frequencies 10
4.2 Calculation of Eigen-Vectors 12
4.3 Measurement of Eigen-Frequencies 14

5 Response to Seismic Motion **15**
5.1 Position Transfer Function 15
5.2 Pitch Transfer Function 16
5.3 Yaw Transfer Function 16

6 Electronic Damping **17**
6.1 Negative Feedback Control System 17
6.2 Constraint dynamics 18
6.3 LIGO Suspension Control System 20

7 Numerical Modeling of Mirror Motion **23**
7.1 Modeling in Matlab 23
7.2 Suppression of Angular Motion 23
7.3 Modeling in E2E 25

Purpose

This document describes dynamical properties of LIGO suspended mirrors for both Large Optics Suspension (LOS) and Small Optics Suspension (SOS). The analysis includes the analytical model and computer simulations, which can be used for experimental studies of the motion of the LIGO suspended mirrors.

Scope

This document includes:

- equations of motion for the suspended mirror,
- eigen-modes and eigen-frequencies of the mirror oscillations,
- analysis of couplings and constraints in the mirror dynamics,
- analysis of electronic damping of the suspended mirrors.

The analytical model described in this document is limited to the motion of the mirror as a rigid body. Vibrations of the suspension wires and elastic deformations of the mirror are not included. These effects are addressed in other (more complicated) models [1, 2].

Relevant Documents

The following LIGO technical documents have related material:

1. S. Kawamura, *Response of pendulum to arbitrary motion of suspension point* [3],
2. S. Kawamura, *Small Optics Suspension Final Design (Mechanical System)* [4],
3. S. Kawamura, *Large Optics Suspension Final Design (Mechanical System)*, [5],
4. H. Yamamoto et al, *End to End Simulation Program for Gravitational Wave Detectors* [6],
5. G. Cella, *Mechanical Simulation Engine: User's Manual* [2],
6. S. Mohanty, *A Formalism for Simulating the SEI/SUS System in the LIGO E2E Model* [1],
7. E. Black et al, *Output Matrix Tuning for Large and Small Optics Controllers* [7],
8. D. Ottaway and M. Landry, *Summary of Mechanical Resonances in the LIGO Hanford Interferometers* [8].

1 Suspension Dimensions

The notations for various dimensions of the suspended mirror are shown in Figure 1. Numerical values for the dimensions of LIGO Large Optics Suspension and Small Optics Suspension are given in Table 1.

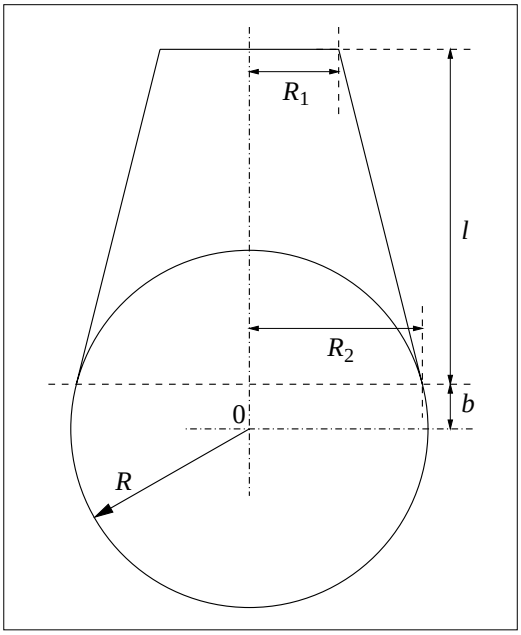

Figure 1: Notations for the dimensions of the suspended mirror.

Table 1: Numerical values for the dimensions of the suspended mirror.

parameter	Large Optics	Small Optics	units
R	0.125	0.038	m
R_1	1.67×10^{-2}	7.92×10^{-3}	m
R_2	0.126	3.80×10^{-2}	m
H	0.10	0.025	m
l	0.442	0.248	m
b	6.83×10^{-3}	9.85×10^{-4}	m

Moments of inertia of a cylinder with radius R and height H are

$$I_1 = \frac{1}{2} m R^2, \tag{1}$$

$$I_2 = \frac{1}{12} m \left(3R^2 + H^2\right), \tag{2}$$

where I_1 corresponds to the rotation around the axis of symmetry, and I_2 corresponds to the rotation around the axis perpendicular to its axis of symmetry. Both axes originate at the center of mass. The mirror mass and its moments of inertia are given in Table 2.

Table 2: Mirror mass and moments of inertia

parameter	Large Optics	Small Optics	units
m	10.5	0.24	kg
I_1	8.2×10^{-2}	1.72×10^{-4}	kg m^2
I_2	4.98×10^{-2}	9.78×10^{-5}	kg m^2

2 Types of Motion

2.1 Degrees of Freedom

The suspended mirror as a rigid body has six degrees of freedom: three for translational and three for rotational motion of the mirror. Three translational degrees of freedom of the mirror are usually the Cartesian coordinates of its center of mass: x, y and z. Three rotational degrees of freedom can be some angles associated with the mirror. Note that Euler angles which are commonly used in mechanics cannot be used to describe rotational motion of the suspended mirror. Infinitesimal Euler angles are linearly-related and therefore do not constitute a set of independent degrees of freedom.

An alternative choice is to use the spherical angles: θ and ϕ of the mirror normal and ψ - the angle of rotation along the normal. The spherical angles define the direction of the normal according to the standard formulas:

$$n_x = \cos\theta\cos\phi, \tag{3}$$
$$n_y = \cos\theta\sin\phi, \tag{4}$$
$$n_z = \sin\theta. \tag{5}$$

Here θ is the angle of elevation of the normal above the horizontal (xy) plane, and ϕ is the angle between the plane of θ-rotations and xz-plane, as shown in Figure 2. These angles are usually small (less than 10^{-2} radians).

A minimal model includes only three coordinates of the mirror. These are - the x-coordinate of the center of mass and the spherical angles: θ and ϕ. The following names for these coordinates are adopted in this document in accordance with the LIGO naming convention:

$$x - \text{position}, \tag{6}$$
$$\theta - \text{pitch}, \tag{7}$$
$$\phi - \text{yaw}. \tag{8}$$

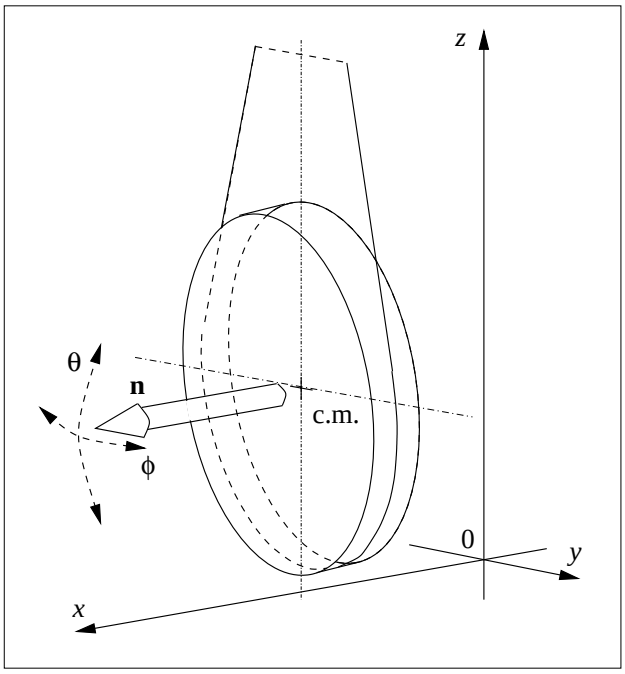

Figure 2: Suspended mirror and the normal vector.

The third angle ψ represents "twist" of the mirror, or the rotation of the mirror around its axis of the symmetry. This degree of freedom is not taken into account in the following model, but can be easily included. Excitation of the mirror by seismic motion is described by translations and rotations of the suspension points, which are denoted by $x_{\rm sp}(t)$ and $\phi_{\rm sp}(t)$.

Due to the symmetry of the suspension and the mirror with respect to zx-plane the yaw-angle decouples from the position and pitch. Therefore there are two independent types of motion: planar motion (x and θ are excited) and pure ϕ-rotation as shown in Figures 3 and 4. The dynamics of the suspended mirror is governed by the Lagrangian, which can be obtained by examining the two types of motion separately.

2.2 Planar Motion

This type of motion occurs when the mirror is excited either in position or pitch. During this motion the points on the mirror and the suspension wires move so that they remain in their respective planes which are parallel to the xz-plane. Thus comes the name "planar motion".

Planar motion of the suspended mirror can be parametrized by the two angles: the pitch angle θ and the angle of the wire deflection from the vertical α, as shown in Figure 3. Then the coordinates of the center of mass are given by

$$x = x_{\rm sp} + l\sin\alpha + b\sin\theta, \tag{9}$$

$$z = l + b - l\cos\alpha - b\cos\theta. \tag{10}$$

Since the angles α and θ are usually small the following approximation can be made:

$$x \approx x_{\rm sp} + l\alpha + b\theta, \tag{11}$$

$$z \approx \frac{1}{2}l\alpha^2 + \frac{1}{2}b\theta^2. \tag{12}$$

Planar motion can be described by either α, θ or x, θ. It is preferable to have x as an independent variable because it is directly related to optical path lengths for the laser beam reflected by the mirror. Then the angle α becomes redundant and can be eliminated through the equation:

$$\alpha = \frac{1}{l}(x - x_{\rm sp} - b\theta). \tag{13}$$

Therefore the lift of the center of mass for planar motion is

$$z = \frac{1}{2l}(x - x_{\rm sp} - b\theta)^2 + \frac{1}{2}b\theta^2. \tag{14}$$

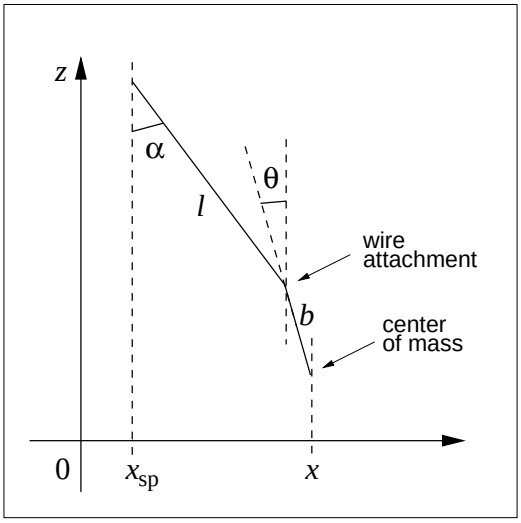

Figure 3: Planar motion of the mirror as viewed from side.

2.3 Pure ϕ-rotations

This type of motion occurs if the mirror rotates in the horizontal plane without lateral motion of its center of mass. (The center of mass moves only in the vertical direction.) In this motion only yaw-angle is excited. Such a motion is generated by the rotation of the suspension $\phi_{\rm sp}(t)$.

As the mirror turns back and forth its center of mass moves up and down. The lift of the center of mass z' can be found as follows. Figure 4 shows that the projection of the wire onto the horizontal plane has the length d, which is defined by

$$d^2 = R_1^2 + R_2^2 - 2R_1R_2\cos(\phi - \phi_{\rm sp}). \tag{15}$$

The length of the wire does not change:

$$l^2 + (R_1 - R_2)^2 = (l - z')^2 + d^2. \tag{16}$$

This equation can be written as the qudratic equation for the lift of the center of mass:

$$z'^2 - 2lz' + 4R_1R_2\sin^2\frac{1}{2}(\phi - \phi_{\rm sp}) = 0. \tag{17}$$

For small rotation angles, z' is small compared to l. Therefore

$$z' \approx \frac{1}{2l}R_1R_2(\phi - \phi_{\rm sp})^2. \tag{18}$$

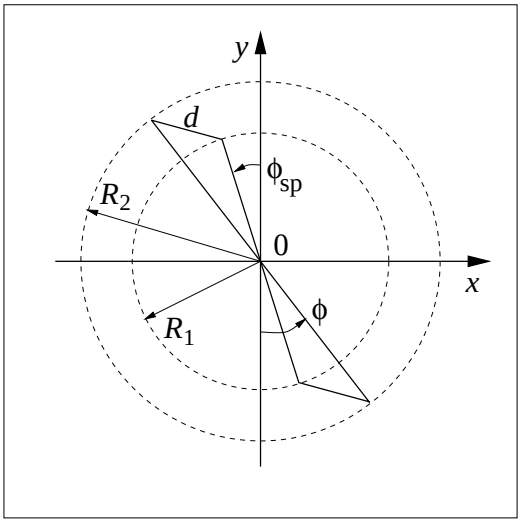

Figure 4: ϕ-rotation of the mirror as viewed from above.

3 Lagrangian for a Suspended Mirror

3.1 Potential Energy

The potential energy of the suspended mirror can be found as

$$U = mg(z + z'), \tag{19}$$

where z and z' are the lifts of the mirror center of mass given by equations (14) and (18). Therefore, the potential energy is

$$U = \frac{mg}{2l}\left[(x - x_{\rm sp} - b\theta)^2 + bl\theta^2 + R_1R_2(\phi - \phi_{\rm sp})^2\right]. \tag{20}$$

3.2 Kinetic Energy

The kinetic energy of the suspended mirror can be found using König's theorem. Namely, if the fixed point of rotation is chosen at the center of mass, the total kinetic energy is a sum of the kinetic energy of translational motion of the center of mass and the kinetic energy of rotations:

$$\mathcal{E}_{\rm kin} = \frac{1}{2}\left[m\dot{x}^2 + I_\theta\dot{\theta}^2 + I_\phi\dot{\phi}^2\right], \tag{21}$$

where I_θ and I_ϕ are the principal moments of inertia of the mirror. Due to the symmetry of the mirror the two principal moments of inertia are equal:

$$I_\theta = I_\phi = I_2, \tag{22}$$

where I_2 is given by Equation (2).

3.3 Lagrangian

The Lagrangian is defined as the difference between the kinetic and the potential energy:

$$\mathcal{L} = \mathcal{E}_{\rm kin} - U. \tag{23}$$

It is a complicated function of x, θ and ϕ:

$$\begin{aligned}\mathcal{L} \;=\; & \frac{1}{2}m\dot{x}^2 + \frac{1}{2}I_\theta\dot{\theta}^2 + \frac{1}{2}I_\phi\dot{\phi}^2 - \\ & \frac{mg}{2l}(x - x_{\rm sp} - b\theta)^2 - \\ & \frac{1}{2}mgb\theta^2 - \frac{1}{2l}mgR_1R_2(\phi - \phi_{\rm sp})^2.\end{aligned} \tag{24}$$

The equations of motion of a suspended mirror as a rigid body are the Euler-Lagrange equations:

$$\frac{d}{dt}\left(\frac{\partial\mathcal{L}}{\partial\dot{q}_i}\right) = \frac{\partial\mathcal{L}}{\partial q_i}, \tag{25}$$

where q_i stands for any of the coordinates x, θ and ϕ.

3.4 Equations of Motion

In the explicit form, the Euler-Lagrange equations for a suspended mirror as a rigid body are

$$m\,\ddot{x} = -m\frac{g}{l}(x - x_{\rm sp} - b\theta), \tag{26}$$

$$I_\theta\,\ddot{\theta} = -mgb\theta + mg\frac{b}{l}(x - x_{\rm sp} - b\theta), \tag{27}$$

$$I_\phi\,\ddot{\phi} = -mR_1R_2\frac{g}{l}(\phi - \phi_{\rm sp}). \tag{28}$$

From these equations we can read the natural frequencies of free oscillations of the mirror:

$$\omega_x^2 = \frac{g}{l}, \tag{29}$$

$$\omega_\theta^2 = \frac{mg}{I_\theta l}b(l+b), \tag{30}$$

$$\omega_\phi^2 = \frac{mg}{I_\phi l}R_1R_2. \tag{31}$$

These natural frequencies correspond to their respective degree of freedom and therefore can be called position, pitch and yaw frequency. Numerical values for natural frequencies of LIGO small and large optics suspension are given in Table 3.

Table 3: Natural frequencies of mirror oscillations (Hz)

frequency	Small Optics	Large Optics
$\omega_x/2\pi$	1.001	0.750
$\omega_\theta/2\pi$	0.773	0.603
$\omega_\phi/2\pi$	0.856	0.500

The above equations describe the motion of the suspended mirror in the absence of friction. In reality suspended mirrors experience some friction. Assume for simplicity that the friction is of the form of viscous damping[1]. Adding the corresponding friction terms we obtain the following equations of motion for the suspended mirror:

$$\ddot{x} + \gamma_x\,\dot{x} + \omega_x^2\,x = \omega_x^2\,(x_{\rm sp} + b\theta), \tag{32}$$

$$\ddot{\theta} + \gamma_\theta\,\dot{\theta} + \omega_\theta^2\,\theta = \frac{\omega_\theta^2}{l+b}(x - x_{\rm sp}), \tag{33}$$

$$\ddot{\phi} + \gamma_\phi\,\dot{\phi} + \omega_\phi^2\,\phi = \omega_\phi^2\,\phi_{\rm sp}. \tag{34}$$

These equations describe small (damped) oscillations of the suspended mirror caused by the motion of its suspension points.

[1]Due to the strong resonance behavior of the suspended mirror the structural damping does not significantly modify the present analysis

Note that the natural frequencies defined in equations (29)-(31) are not usually observed, except for ω_ϕ. The observed frequencies are eigen-frequencies of the mirror oscillations. These are found next.

4 Eigen-Modes of Mirror Oscillations

4.1 Calculation of Eigen-Frequencies

To study frequency response of the suspended mirror apply Laplace transformation to these equations. The eigen-modes of the motion of the suspended mirror correspond to the complex values of the parameter s:

$$s_j = -\Gamma_j + i\Omega_j, \tag{35}$$

for $j = 1, 2, 3$. Here Ω_j are the eigen-frequencies and Γ_j are the corresponding damping coefficients. These eigen-values can be found by studying the frequency response of the suspended mirror.

Planar Motion

The first two equations which describe the planar motion of the suspended mirror can be written in a matrix form:

$$\mathbf{P}(s) \begin{bmatrix} \tilde{x}(s) \\ \\ \tilde{\theta}(s) \end{bmatrix} = \tilde{x}_{\rm sp}(s) \begin{bmatrix} \omega_x^2 \\ \\ -\omega_\theta^2/(l+b). \end{bmatrix}, \tag{36}$$

where $\mathbf{P}(s)$ is the 2×2-matrix defined as

$$\mathbf{P}(s) = \begin{pmatrix} s^2 + \gamma_x s + \omega_x^2 & -b\,\omega_x^2 \\ \\ -\omega_\theta^2/(l+b) & s^2 + \gamma_\theta s + \omega_\theta^2 \end{pmatrix}. \tag{37}$$

The eigen-values of the planar motion can be found by solving the equation:

$$\det \mathbf{P}(s) = 0. \tag{38}$$

There are four solutions to this equation: s_1, s_2 and s_1^*, s_2^*. If these eigen-values are known, the determinant of the matrix $\mathbf{P}(s)$ can be written in the factorized form:

$$\det \mathbf{P}(s) = (s - s_1)(s - s_1^*)(s - s_2)(s - s_2^*). \tag{39}$$

In general, there are no simple formulas for these eigen-values. However, for small damping we can obtain approximate formulas for the eigen-values. Then the formula for the eigen-frequencies is

$$\Omega_{1,2}^2 \approx \frac{g}{2l}\left[1 + \frac{mb(l+b)}{I_\theta} \mp \sqrt{\left[1 - \frac{mb(l+b)}{I_\theta}\right]^2 + 4\frac{mb^2}{I_\theta}}\,\right]. \tag{40}$$

The corresponding damping coefficients can also be found approximately:

$$\Gamma_{1,2} \approx \frac{1}{4}(\gamma_x + \gamma_\theta) \mp \frac{1}{4}(\gamma_x - \gamma_\theta)\frac{1 - \frac{mb(l+b)}{I_\theta}}{\sqrt{\left[1 - \frac{mb(l+b)}{I_\theta}\right]^2 + 4\frac{mb^2}{I_\theta}}}. \tag{41}$$

Since LIGO suspensions have very high quality factors the damping coefficients γ_x and γ_θ are very small (in comparison to critical damping) and the above approximation holds very well.

Consider a special case:

$$b \ll l, \quad \text{and} \quad \frac{mb(l+b)}{I_\theta} \ll 1. \tag{42}$$

Then the following condition takes place:

$$\frac{mb^2}{I_\theta} \ll 1. \tag{43}$$

In this case the eigen-frequencies can be approximated as follows:

$$\Omega_1^2 \approx \omega_\theta^2 \left[1 - \frac{(b/l)}{1 - \omega_\theta^2/\omega_x^2}\right], \tag{44}$$

$$\Omega_2^2 \approx \omega_x^2 \left[1 - \frac{(mb^2/I_\theta)}{1 - \omega_\theta^2/\omega_x^2}\right]. \tag{45}$$

These formulas show that

$$\Omega_1 \to \omega_\theta, \quad \text{and} \quad \Omega_2 \to \omega_x. \tag{46}$$

Note that the limiting formulas, Equations (44) and (45), should be used with care. Although the first condition ($b \ll l$) is satisfied, the second condition ($mb(l+b)/I_\theta \ll 1$) is not.

Pure ϕ-rotation

Laplace-domain equation which describes ϕ-rotations of the mirror is

$$(s^2 + \gamma_\phi\, s + \omega_\phi^2)\ \tilde{\phi}(s) = \omega_\phi^2\ \tilde{\phi}_{\rm sp}(s). \tag{47}$$

This motion is an eigen-mode of the suspended mirror and its eigen-value is

$$s_3 = -\frac{\gamma_\phi}{2} + i\sqrt{\omega_\phi^2 - \frac{\gamma_\phi^2}{4}}. \tag{48}$$

Separating the real and imaginary parts of this eigen-value we obtain:

$$\Omega_3 = \sqrt{\omega_\phi^2 - \gamma_\phi^2/4} \approx \omega_\phi, \tag{49}$$

$$\Gamma_3 = \gamma_\phi/2. \tag{50}$$

4.2 Calculation of Eigen-Vectors

There are two eigen-vectors for planar motion of the suspended mirror:

$$\mathbf{E}_j = \mathrm{const} \begin{bmatrix} 1 \\ (s_j^2 + \gamma_x s_j + \omega_x^2)/\omega_x^2 b \end{bmatrix}, \tag{51}$$

where $j = 1, 2$. These eigen-vectors correspond to the two eigen-values:

$$s_j = -\Gamma_j + i\Omega_j, \tag{52}$$

where Ω_j and Γ_j are given by Equations (40) and (41).

The eigen-vectors are defined up to a multiplicative constant. To be specific consider the eigen-vectors which correspond to 1μm of displacement of the center of mass:

$$\mathrm{const} = 1\ \mu\mathrm{m}. \tag{53}$$

Then the eigen-vectors for the small optics suspension are:

$$\mathbf{E}_1 = \begin{bmatrix} 1\ \mu\mathrm{m} \\ (415.90 + i\ 0.02)\ \mu\mathrm{rad} \end{bmatrix}, \quad \mathbf{E}_2 = \begin{bmatrix} 1\ \mu\mathrm{m} \\ -(697.72 + i\ 0.04)\ \mu\mathrm{rad} \end{bmatrix}, \tag{54}$$

Corresponding eigen-vectors for the large optics suspension are:

$$\mathbf{E}_1 = \begin{bmatrix} 1\ \mu\mathrm{m} \\ (55.515 + i\ 0.002)\ \mu\mathrm{rad} \end{bmatrix}, \quad \mathbf{E}_2 = \begin{bmatrix} 1\ \mu\mathrm{m} \\ -(85.832 + i\ 0.004)\ \mu\mathrm{rad} \end{bmatrix}, \tag{55}$$

The eigen-vectors are complex, which is a consequence of dissipation. Schematic diagram of the mirror motion corresponding to these two eigen-vectors is shown in Figure 5.

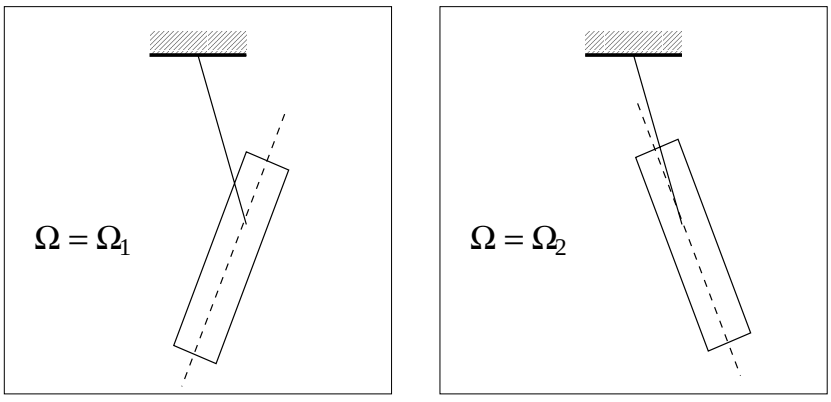

Figure 5: Eigen-modes of planar motion.

Free motion of the mirror in the planar mode can be described in terms of these eigenvectors as follows:

$$\begin{bmatrix} x(t) \\ \\ \theta(t) \end{bmatrix} = \mathrm{Re}\left\{ c_1 \ \mathbf{E}_1 \ e^{s_1 t} + c_2 \ \mathbf{E}_2 \ e^{s_2 t} \right\}. \tag{56}$$

where c_1 and c_2 are arbitrary complex numbers.

Yaw-motion of the mirror is an eigen-mode. Therefore, free motion of the mirror in the ϕ-rotation mode can be described as follows:

$$\phi(t) = \mathrm{Re}\left\{ c_3 \ e^{s_3 t} \right\}. \tag{57}$$

where c_3 is an arbitrary complex number.

4.3 Measurement of Eigen-Frequencies

The eigen-frequencies can be found from the measurements of power spectral density of any of the sensor signals of the suspended optics. A typical power spectral density is shown in Figure 6.

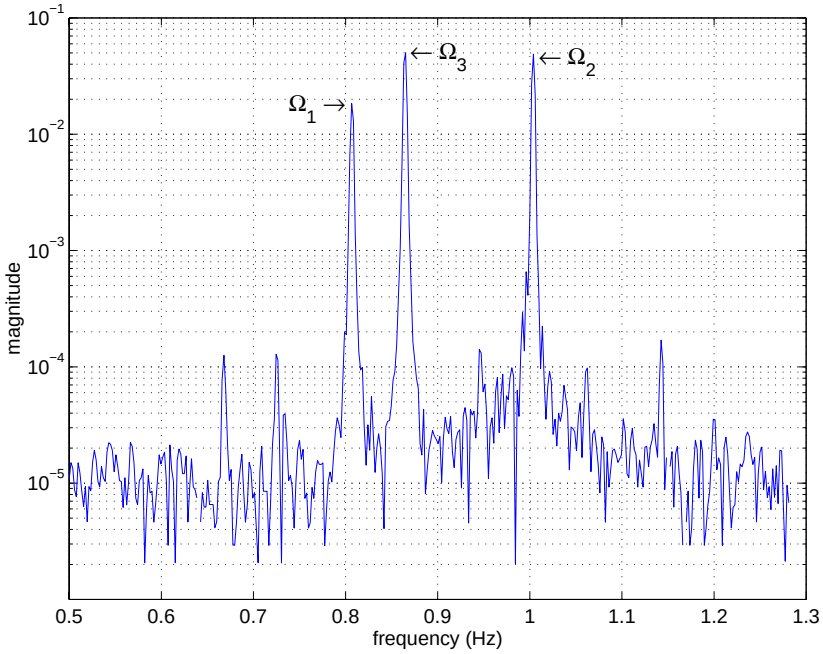

Figure 6: Power spectral density of one of the sensor outputs of LIGO small optics suspension.

The measurements eigen-frequencies and the calculations based on equations (40,41), and (49,50), are shown in Table 4. The error in the measurement is typically a millihertz.

Table 4: Eigen-frequencies of mirror oscillations (Hz)

	Small Optics		Large Optics	
frequency	(theory)	(exper.)	(theory)	(exper.)
$\Omega_1/2\pi$	0.769	0.806	0.591	0.627
$\Omega_2/2\pi$	1.004	1.004	0.759	0.760
$\Omega_3/2\pi$	0.856	0.865	0.499	0.507

The measured eigen-frequencies of small optics are obtained from the power spectral density (Figure 6). The measured eigen-frequencies of the large optics are taken from [9]. (They correspond to MMT3 of LIGO LLO.) The eigen-frequencies of LIGO optics measured at LIGO LHO can be found in [8].

5 Response to Seismic Motion

The response of the suspended mirror to the seismic motion is described in terms of Laplace-domain transfer functions.

5.1 Position Transfer Function

The translational motion of the suspension point excites the position of the center of mass:

$$\tilde{x}(s) = H_x(s)\ \tilde{x}_{\rm sp}(s), \tag{58}$$

where $H_x(s)$ is the position transfer function. Inverting the matrix in Equation (36) we find that this transfer function is given by

$$H_x(s) = \frac{\omega_x^2(s^2 + \gamma_x s + \omega_b^2)}{(s - s_1)(s - s_1^*)(s - s_2)(s - s_2^*)}, \tag{59}$$

where ω_b is given by

$$\omega_b = \sqrt{\frac{mgb}{I_\theta}}. \tag{60}$$

A Bode plot of this transfer function is shown in Figure 7. This transfer function has four

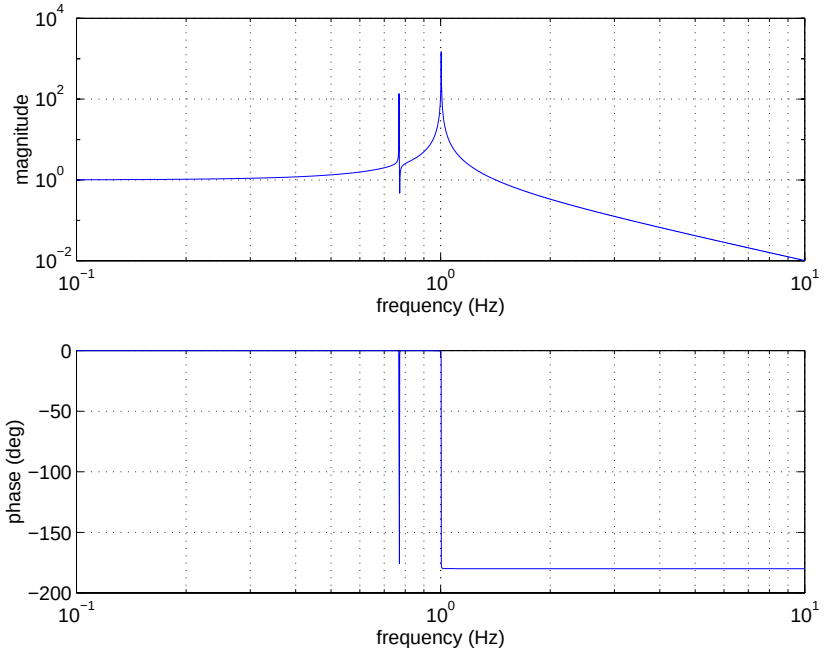

Figure 7: Bode plot of "position" transfer function, $H_x(s)$.

poles and two zeros. Each complex pole appears in pair with its complex conjugate. The pairs of the complex conjugate poles correspond to the resonances in the motion of the

suspended mirror. The frequencies of the resonances are equal to the eigen-frequencies of the planar motion $\Omega_{1,2}$. The widths of the resonances are defined by the corresponding damping coefficients $\Gamma_{1,2}$.

The transfer function also has a pair of complex conjugate zeros:

$$s \approx -\frac{\gamma_x}{2} \pm i\omega_b. \tag{61}$$

The zeros give rise to a cusp in the transfer function at the frequency ω_b. Such zeros in the transfer function correspond to a "node", which appears at the location of the mirror's center of mass. Note that for any choice of suspension parameters the frequency of the zero always lies between the two eigen-frequencies:

$$\Omega_1 < \omega_b < \Omega_2. \tag{62}$$

5.2 Pitch Transfer Function

The translational motion of the suspension point also excites pitch angle of the mirror:

$$\tilde{\theta}(s) = -H_\theta(s)\ \frac{\tilde{x}_{\rm sp}(s)}{l+b}, \tag{63}$$

where $H_\theta(s)$ is the corresponding transfer function. The minus sign reflects our choice of coordinates: the motion of the suspension point which causes the mirror to move forward ($x > 0$) tilts the normal $\vec{n}$ down ($\theta < 0$). Inverting the matrix in Equation (36), we find that this transfer function is given by

$$H_\theta(s) = \frac{\omega_\theta^2\ s(s+\gamma_\theta)}{(s-s_1)(s-s_1^*)(s-s_2)(s-s_2^*)}. \tag{64}$$

A Bode plot of this transfer function is shown in Figure 8.

The transfer function $H_\theta(s)$ has four poles, which are the same as the poles of $H_x(s)$. It also has two zeros:

$$s = 0, \tag{65}$$

$$s = -\gamma_\theta. \tag{66}$$

The zero of the transfer function at zero-frequency indicates that the pitch angle is AC-coupled. In other words, the pitch angle is insensitive to static displacements of the suspension point.

5.3 Yaw Transfer Function

The ϕ-rotations of the suspended mirror are excited by the rotations of the suspension points:

$$\tilde{\phi}(s) = H_\phi(s)\ \tilde{\phi}_{\rm sp}(s), \tag{67}$$

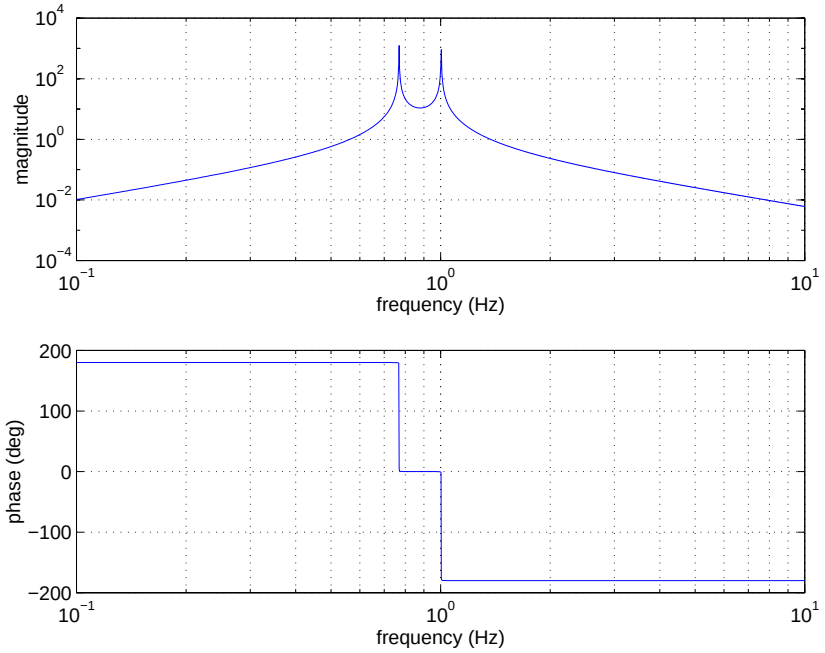

Figure 8: Bode plot of "pitch" transfer function, $H_\theta(s)$.

where $H_\phi(s)$ is the corresponding transfer function:

$$H_\phi(s) = \frac{\omega_\phi^2}{s^2 + \gamma_\phi s + \omega_\phi^2}. \tag{68}$$

This is a typical response of a damped oscillator. The frequency of the complex poles is Ω_ϕ.

6 Electronic Damping

6.1 Negative Feedback Control System

The resonances of oscillations of the suspended mirror are suppressed by a negative feedback control system. The effect of such a control system can be described in the model by adding the control forces $f_j(t)$ to the right-hand side of Equations (32)-(34). The resulting equations of motion are:

$$\ddot{x} + \gamma_x\ \dot{x} + \omega_x^2\ x = \omega_x^2\ (x_{\rm sp} + b\theta) + f_x(t), \tag{69}$$

$$\ddot{\theta} + \gamma_\theta\ \dot{\theta} + \omega_\theta^2\ \theta = \frac{\omega_\theta^2}{l+b}(x - x_{\rm sp}) + f_\theta(t), \tag{70}$$

$$\ddot{\phi} + \gamma_\phi\ \dot{\phi} + \omega_\phi^2\ \phi = \omega_\phi^2\ \phi_{\rm sp} + f_\phi(t). \tag{71}$$

The control forces are formed from the corresponding coordinates by linear transformations (filtering):

$$\tilde{f}_x(s) = -G_1(s)\,\tilde{x}(s), \quad (72)$$
$$\tilde{f}_\theta(s) = -G_2(s)\,\tilde{\theta}(s), \quad (73)$$
$$\tilde{f}_\phi(s) = -G_3(s)\,\tilde{\phi}(s). \quad (74)$$

where $G_j(s)$ are the transfer functions of the control system.

A slight complication in LIGO suspension control systems arises from the fact that there are four sensor signals to monitor the three degrees of freedom: one signal too many. It also uses four actuators to apply forces to the mirror. As a result a constraint occurs in the dynamics of a suspended mirror. This constraint and the technique to overcome it is discussed below.

6.2 Constraint dynamics

For small mirror oscillations the relation between the mirror degrees of freedom and the sensor signals is linear. This linear relation is described by the sensor matrix, which can be introduced as follows. A suspended mirror in LIGO has four magnets attached to one of its sides near the mirror perimeter. Each mirror degree of freedom produces the following displacements of the magnets:

$$x_1 = x, \quad (75)$$
$$x_2 = R_m\theta, \quad (76)$$
$$x_3 = R_m\phi \quad (77)$$

where R_m is the length of the lever of a magnet[2]. (R_m is the half-distance between the adjacent magnets.)

Then the coordinates of the four magnets along the x-axis are:

$$m_1 = x_1 + x_2 + x_3, \quad (78)$$
$$m_2 = x_1 + x_2 - x_3, \quad (79)$$
$$m_3 = x_1 - x_2 - x_3, \quad (80)$$
$$m_4 = x_1 - x_2 + x_3. \quad (81)$$

These coordinates are sensed by the photodiode-LED pairs set near each magnet. After calibration the sensor voltages become the coordinates of the four magnets.

Since there are only three degrees of freedom these four sensor voltages are not independent. There is a constraint:

$$m_1 - m_2 + m_3 - m_4 = 0, \quad (82)$$

which means that all four magnets remain in a plane for arbitrary motion of the mirror. In other words, there is no bending of the mirror surface.

[2]For LIGO LOS $R_m = 0.085$ m.

The inverse transformation relates the mirror degrees of freedom to the sensor voltages and is given by the following equations:

$$x_1 = (m_1 + m_2 + m_3 + m_4)/4, \quad (83)$$
$$x_2 = (m_1 + m_2 - m_3 - m_4)/4, \quad (84)$$
$$x_3 = (m_1 - m_2 - m_3 + m_4)/4. \quad (85)$$

The constraint makes it difficult to analyze the dynamics of the suspended mirror with the control system. One of the standard techniques to overcome this difficulty is to "lift" the constraint. This is done by introducing a new degree of freedom,

$$x_4 = (m_1 - m_2 + m_3 - m_4)/4, \quad (86)$$

which becomes the fourth coordinate of the mirror. (More about lifting a constraint can be found in the theory of constraint dynamic systems.)

The coordinate x_4 does not correspond to any motion of the mirror: it is a measure of how much the mirror is bent. After introduction of this new coordinate Equations (83) - (86) can be written in the matrix form:

$$\mathbf{x}(t) = \frac{1}{4}\mathbf{U}\ \mathbf{m}(t), \quad (87)$$

where $\mathbf{U}$ is a 4×4-matrix

$$\mathbf{U} = \begin{pmatrix} 1 & 1 & 1 & 1 \\ 1 & 1 & -1 & -1 \\ 1 & -1 & -1 & 1 \\ 1 & -1 & 1 & -1 \end{pmatrix}. \quad (88)$$

This matrix is non-degenerate and therefore can be inverted. Moreover, it has a remarkable property of being proportional to its inverse:

$$\mathbf{U}^{-1} = \frac{1}{4}\mathbf{U}, \quad (89)$$

Therefore,

$$\frac{1}{4}\mathbf{U}\ \mathbf{U} = \mathbf{1}, \quad (90)$$

where $\mathbf{1}$ is the unit matrix. This property can also be seen from Equations (78) - (81) which can be written now in terms of the matrix $\mathbf{U}$:

$$\mathbf{m}(t) = \mathbf{U}\ \mathbf{x}(t). \quad (91)$$

Thus the matrix $\mathbf{U}$ transforms the mirror degrees of freedom to sensor voltages and vice versa.

In practice the four sensors (LED-photodiode pairs) have slightly different sensitivity and therefore produce slightly different voltages for the same mirror displacement. Calibration of the sensor is done in the suspension control system by adjusting the values of the input matrix.

Similarly, the four actuators (coil-magnet pairs) have slightly different strength and therefore produce slightly different mirror displacement for the same current. This inequality is corrected by the output matrix of the suspension control system. A description of some calibration procedures can be found in [7].

The suspension control system is implemented in LIGO using EPICS control interface. A snapshot of the EPICS screen is shown in Figure 9.

6.3 LIGO Suspension Control System

The transformations of the signals which take place in the suspension controller can be broken into four steps as follows:

1. The four photodiode-LED pairs form the four sensor signals m_j. These four signals are converted into the following four voltages:

$$\tilde{\mathbf{x}}'(s) = \frac{1}{4}\mathbf{U}\ \tilde{\mathbf{m}}(s), \tag{92}$$

   which, in principle, are equivalent[3] to the four mirror degrees of freedom, x_j.

2. The four voltages serve as an input for the control system electronics which produce the following four error correction signals:

$$\tilde{\mathbf{C}}(s) = \mathbf{G}\ \tilde{\mathbf{x}}'(s), \tag{93}$$

   where $\mathbf{G}(s)$ is the control system matrix:

$$\mathbf{G}(s) = \begin{pmatrix} G_1(s) & & & \\ & G_2(s) & & \\ & & G_3(s) & \\ & & & 0 \end{pmatrix}. \tag{94}$$

   Note that the error-correction signal which corresponds to the fourth degree of freedom must be zero.

3. The error-correction signals are transformed into four actuator voltages:

$$\tilde{\mathbf{V}}(s) = -\mathbf{U}\ \tilde{\mathbf{C}}(s), \tag{95}$$

   which are sent to the four electromagnetic coils mounted to the suspension frame. Each coil acts on its corresponding magnet through the magnetic field to produce a force on the mirror.

4. Linear combinations of these four forces give rise to the net force affecting the mirror center of mass, the torques affecting the angular degrees of freedom, and the

[3] Such equivalence is accurate for mirror displacements, which are within the linear range of the photodiodes.

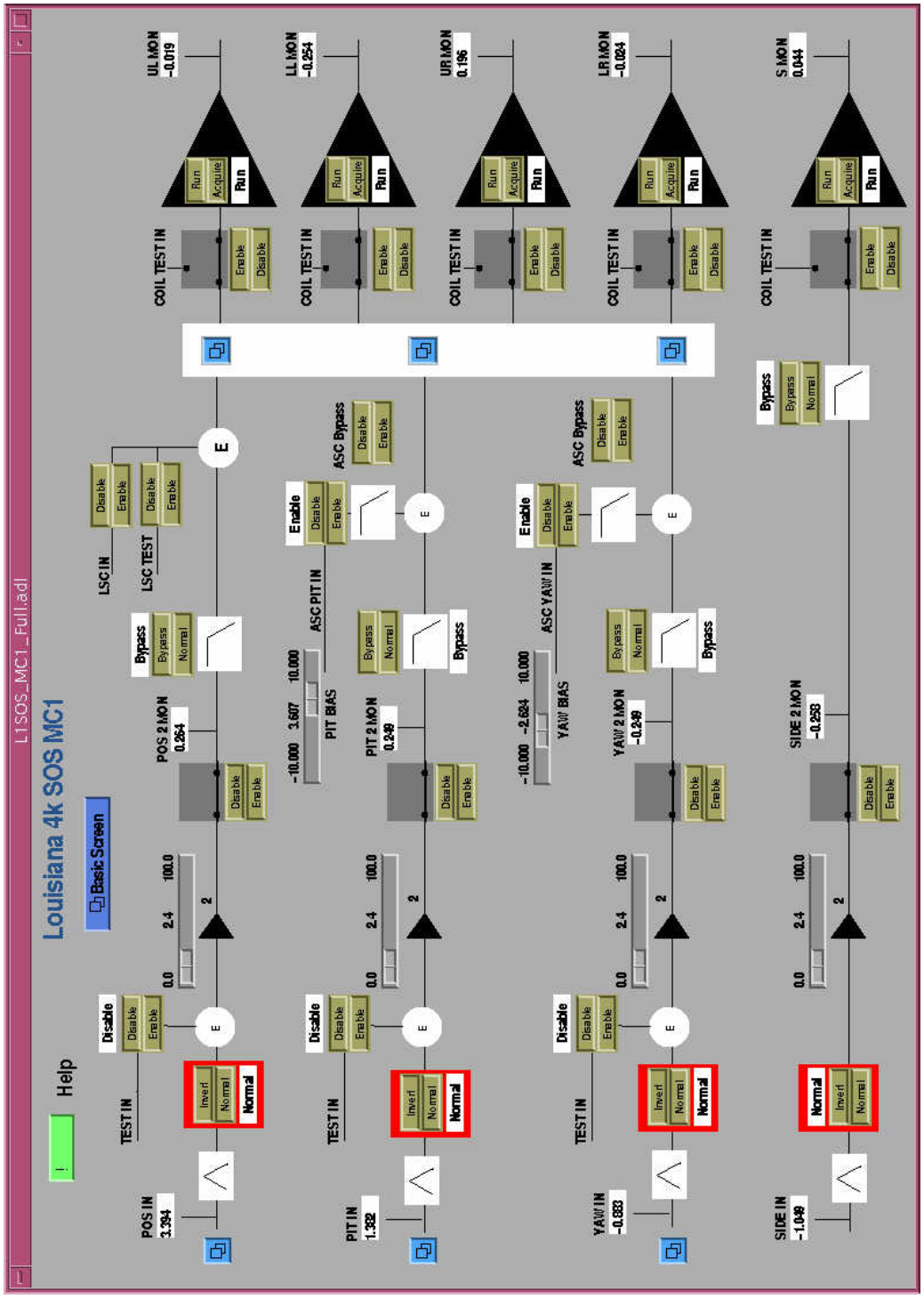

Figure 9: A snapshot of EPICS screen of LIGO suspension control system.

stress affecting the bending mode. All of them can be written as the generalized forces:

$$\tilde{\mathbf{f}}(s) = \frac{1}{4}\mathbf{U}\ \tilde{\mathbf{V}}(s). \tag{96}$$

This completes the loop of the negative feedback.

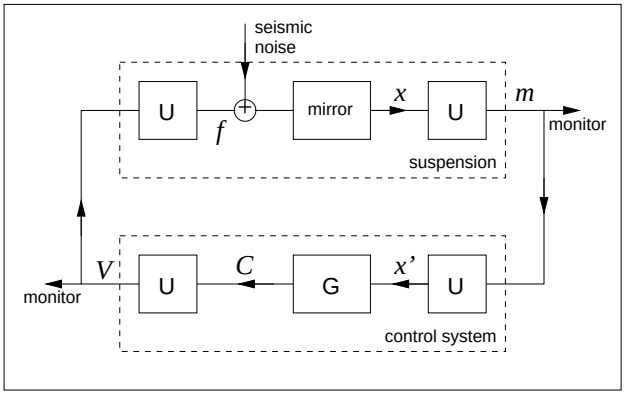

Figure 10: Block diagram of LIGO suspension control system.

The signals and the transformations of the feedback loop are shown schematically in Figure 10. The combined effect of all the elements in the feedback is described by the following formula:

$$\tilde{\mathbf{f}}(s) = -\left[\frac{1}{4}\mathbf{U}\ \mathbf{U}\ \tilde{\mathbf{G}}(s)\frac{1}{4}\mathbf{U}\right]\ \tilde{\mathbf{m}}(s) \tag{97}$$

$$= -\tilde{\mathbf{G}}(s)\ \tilde{\mathbf{x}}(s). \tag{98}$$

Thus the result is the same as if the control forces f_j were formed directly from the mirror coordinates x_j.

7 Numerical Modeling of Mirror Motion

7.1 Modeling in Matlab

There are several models in LIGO which are developed for simulation of motion of the suspended mirror driven by the seismic noise and the control system. The simplest of them is the model based on the Lagrangian approach described in this document. In this model the equations of mirror motion, (69-71), are expressed in terms of digital filters. Such a model is written in Matlab as a part of LIGO End-to-End (E2E) model development [10].

The model generates time-domain evolution of the three degrees of freedom: position, pitch and yaw. The input to the model is the initial mirror coordinates and the velocities. The simulated mirror trajectory is then obtained by iterating the digital-filter transformations with the time step small compared to the periods of the mirror resonances. An example of the simulated mirror motion is shown in Figure 11 (left diagram). For comparison, an oscilloscope trace of the real mirror motion is shown in the same Figure (right diagram).

This model is also implemented as a "primitive module" in the E2E model. A brief description of the module and an example of the simulation of mirror motion in the E2E are given below.

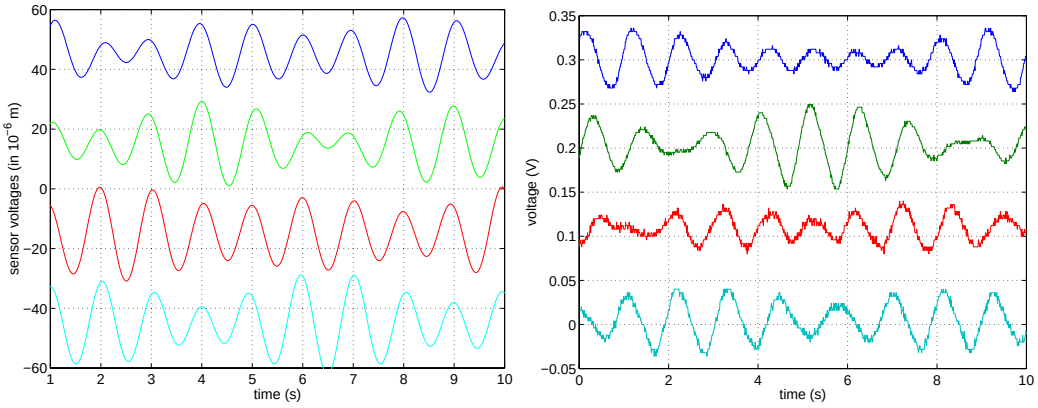

Figure 11: Sensor voltages for a typical mirror motion: simulation *(left)* and measurement *(right)*.

7.2 Suppression of Angular Motion

One of the applications of the model is the study of the dynamic coupling of the degrees of freedom of the suspended mirror. For example, one can analyze various consequences of the "position-pitch" coupling.

Often only the angular degrees of freedom are damped; the translational motion of the mirror is left free. This is done by turning off the electronic damping which corresponds to the translational motion of the mirror ($G_1(s) = 0$). Since the mirror coordinates are

coupled the separation of the translation motion of the mirror from its angular motion is not complete. Here we discuss the effect of this coupling in the presence of the control system using numerical solutions of the equations for mirror motion.

The result of the numerical simulations is shown in Figure 12. The motion is excited by the initial conditions which were chosen away from equilibrium. Both θ and ϕ are damped by the suspension control electronics. In each case the damping is close to critical.

Consider the damped oscillations of the angle θ in Figure 12. Note that the first part of the curve $\theta(t)$ shows that the control system suppressed the oscillations caused by the initial conditions (large deviation from equilibrium). At the same time θ is excited by the translational motion of the mirror which is not directly suppressed. Thus the magnitude of the residual motion of the mirror is defined not only by the gain of the control system but also by the magnitude of the translational motion of the mirror and the position-pitch coupling.

Consider the oscillations of the mirror position in Figure 12. Note that these oscillations are also damped. Although there is no direct damping of the translational motion of the mirror the damping appears indirectly - through the position-pitch coupling. Therefore the translational motion of the mirror is not entirely free if the pitch angle is damped.

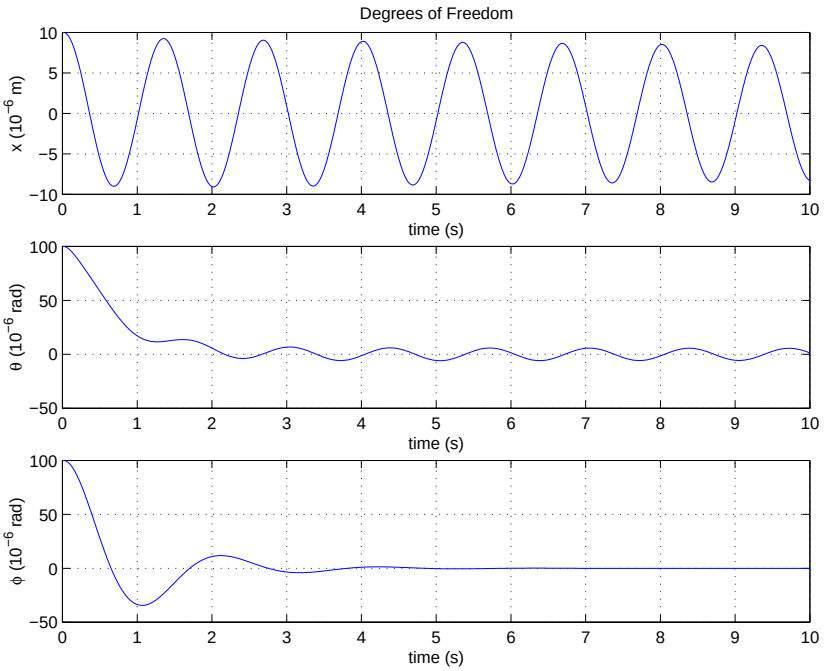

Figure 12: Damped motion of a suspended mirror.

7.3 Modeling in E2E

The suspended mirror as a rigid body is implemented in E2E as a primitive, which can be called from the Alfi graphical user interface. The notations for the parameters and the settings of the Rigid Body primitive in E2E are different from those used in this text. They correspond to the convention adopted in [4, 5] and are shown in Figure 13.

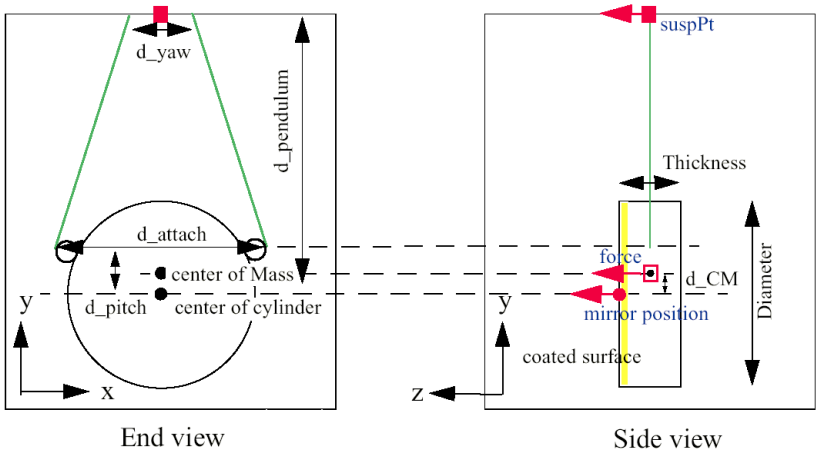

Figure 13: Dimensions of suspended mirror in End-to-End model

Snapshots of the E2E box-diagrams are shown in Figures 14 and 15. One of the many results of the modeling motion of the suspended mirror with E2E is shown in Figure 16. In this Figure, the upper diagram shows a sample of the time-domain simulations for the two degrees of freedom (position and pitch), the lower diagram shows the corresponding transfer functions. These transfer function are similar to the ones obtained in analytical model, Equations (59) and (64).

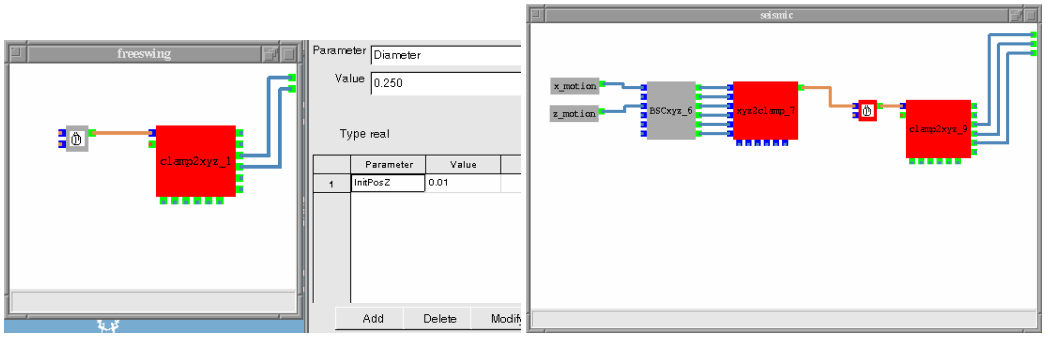

Figure 14: The E2E primitive *(left)* and the E2E Box *(right)* to generate seismic motion of the suspended mirror.

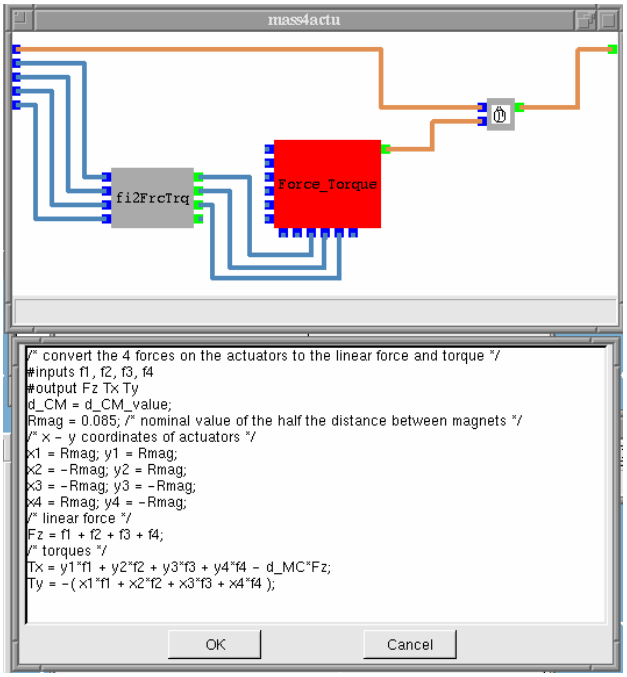

Figure 15: E2E Box containing the Rigid Body and the Box with generalized forces.

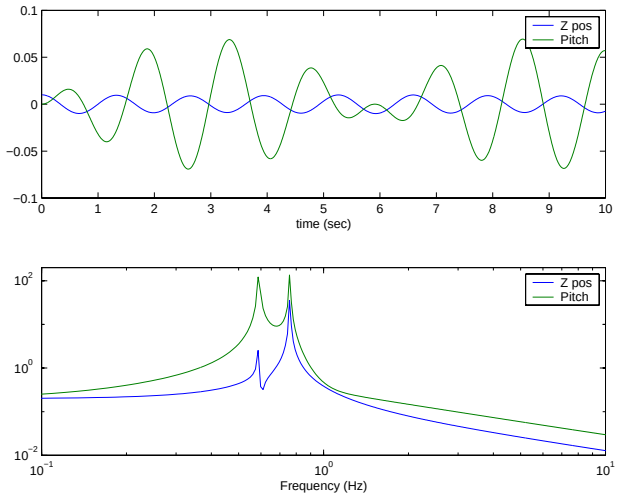

Figure 16: Mirror motion simulated with E2E and the corresponding transfer functions

References

[1] S. Mohanty. A formalism for simulating the SEI/SUS system in the LIGO E2E model. LIGO technical report T990014, California Institute of Technology, Pasadena, California, 1999.

[2] G. Cella. Mechanical simulation engine: User's manual. LIGO technical report T990107, California Institute of Technology, Pasadena, California, 1999.

[3] S. Kawamura. Response of pendulum to arbitrary motion of suspension point. LIGO technical report T960040, California Institute of Technology, Pasadena, California, 1996.

[4] S. Kawamura and J. Hazel. Small optics suspension final design (mechanical system). LIGO technical report T970135, California Institute of Technology, Pasadena, California, 1997.

[5] S. Kawamura, J. Hazel, and M. Barton. Large optics suspension final design (mechanical system). LIGO technical report T970158, California Institute of Technology, Pasadena, California, September 1997.

[6] Yamamoto et al. End to end simulation program for gravitational wave detectors. LIGO technical report P000018, California Institute of Technology, Pasadena, California, October 2000.

[7] E. Black, G. Gonzales, N. Mavalvala, and D. Shoemaker. Output matrix tuning for large and small optics controllers. LIGO technical report T990094, California Institute of Technology, Pasadena, California, November 1999.

[8] D. Ottaway and M. Landry. Summary of mechanical resonances in the ligo hanford interferometers. LIGO technical report T000020, California Institute of Technology, Pasadena, California, September 2000.

[9] W. Johnson, G. Traylor, and S. Yoshida. Suspension survey. LIGO E-log entry, LIGO Livingston Observatory, November 17 2000.

[10] M. Rakhmanov. *Rigid Body* - a Matlab program for simulation of motion of ligo suspended mirror (March 1999). The source code can be obtained from: `www.ligo.caltech.edu/~malik/matlab`.